

Determination of spin and parity of the $Z_c(3900)$

M. Ablikim¹, M. N. Achasov^{9,f}, X. C. Ai¹, O. Albayrak⁵, M. Albrecht⁴, D. J. Ambrose⁴⁴, A. Amoroso^{49A,49C}, F. F. An¹, Q. An^{46,a}, J. Z. Bai¹, R. Baldini Ferroli^{20A}, Y. Ban³¹, D. W. Bennett¹⁹, J. V. Bennett⁵, M. Bertani^{20A}, D. Bettoni^{21A}, J. M. Bian⁴³, F. Bianchi^{49A,49C}, E. Boger^{23,d}, I. Boyko²³, R. A. Briere⁵, H. Cai⁵¹, X. Cai^{1,a}, O. Cakir^{40A,b}, A. Calcaterra^{20A}, G. F. Cao¹, S. A. Cetin^{40B}, J. F. Chang^{1,a}, G. Chelkov^{23,d,e}, G. Chen¹, H. S. Chen¹, H. Y. Chen², J. C. Chen¹, M. L. Chen^{1,a}, S. Chen⁴¹, S. J. Chen²⁹, X. Chen^{1,a}, X. R. Chen²⁶, Y. B. Chen^{1,a}, H. P. Cheng¹⁷, X. K. Chu³¹, G. Cibinetto^{21A}, H. L. Dai^{1,a}, J. P. Dai³⁴, A. Dbeyssi¹⁴, D. Dedovich²³, Z. Y. Deng¹, A. Denig²², I. Denysenko²³, M. Destefanis^{49A,49C}, F. De Mori^{49A,49C}, Y. Ding²⁷, C. Dong³⁰, J. Dong^{1,a}, L. Y. Dong¹, M. Y. Dong^{1,a}, Z. L. Dou²⁹, S. X. Du⁵³, P. F. Duan¹, J. Z. Fan³⁹, J. Fang^{1,a}, S. S. Fang¹, X. Fang^{46,a}, Y. Fang¹, R. Farinelli^{21A,21B}, L. Fava^{49B,49C}, O. Fedorov²³, F. Feldbauer²², G. Felici^{20A}, C. Q. Feng^{46,a}, E. Fioravanti^{21A}, M. Fritsch^{14,22}, C. D. Fu¹, Q. Gao¹, X. L. Gao^{46,a}, X. Y. Gao², Y. Gao³⁹, Z. Gao^{46,a}, I. Garzia^{21A}, K. Goetzen¹⁰, L. Gong³⁰, W. X. Gong^{1,a}, W. Gradl²², M. Greco^{49A,49C}, M. H. Gu^{1,a}, Y. T. Gu¹², Y. H. Guan¹, A. Q. Guo¹, L. B. Guo²⁸, R. P. Guo¹, Y. Guo¹, Y. P. Guo²², Z. Haddadi²⁵, A. Hafner²², S. Han⁵¹, X. Q. Hao¹⁵, F. A. Harris⁴², K. L. He¹, T. Held⁴, Y. K. Heng^{1,a}, Z. L. Hou¹, C. Hu²⁸, H. M. Hu¹, J. F. Hu^{49A,49C}, T. Hu^{1,a}, Y. Hu¹, G. S. Huang^{46,a}, J. S. Huang¹⁵, X. T. Huang³³, X. Z. Huang²⁹, Y. Huang²⁹, Z. L. Huang²⁷, T. Hussain⁴⁸, Q. Ji¹, Q. P. Ji³⁰, X. B. Ji¹, X. L. Ji^{1,a}, L. W. Jiang⁵¹, X. S. Jiang^{1,a}, X. Y. Jiang³⁰, J. B. Jiao³³, Z. Jiao¹⁷, D. P. Jin^{1,a}, S. Jin¹, T. Johansson⁵⁰, A. Julin⁴³, N. Kalantar-Nayestanaki²⁵, X. L. Kang¹, X. S. Kang³⁰, M. Kavatsyuk²⁵, B. C. Ke⁵, P. Kiese²², R. Kliemt¹⁴, B. Kloss²², O. B. Kolcu^{40B,i}, B. Kopf⁴, M. Kornicer⁴², W. Kuehn²⁴, A. Kupsc⁵⁰, J. S. Lange^{24,a}, M. Lara¹⁹, P. Larin¹⁴, C. Leng^{49C}, C. Li⁵⁰, Cheng Li^{46,a}, D. M. Li⁵³, F. Li^{1,a}, F. Y. Li³¹, G. Li¹, H. B. Li¹, H. J. Li¹, J. C. Li¹, Jin Li³², K. Li¹³, K. Li³³, Lei Li³, P. R. Li⁴¹, Q. Y. Li³³, T. Li³³, W. D. Li¹, W. G. Li¹, X. L. Li³³, X. M. Li¹², X. N. Li^{1,a}, X. Q. Li³⁰, Y. B. Li², Z. B. Li³⁸, H. Liang^{46,a}, J. J. Liang¹², Y. F. Liang³⁶, Y. T. Liang²⁴, G. R. Liao¹¹, D. X. Lin¹⁴, B. Liu³⁴, B. J. Liu¹, C. X. Liu¹, D. Liu^{46,a}, F. H. Liu³⁵, Fang Liu¹, Feng Liu⁶, H. B. Liu¹², H. H. Liu¹⁶, H. H. Liu¹, H. M. Liu¹, J. Liu¹, J. B. Liu^{46,a}, J. P. Liu⁵¹, J. Y. Liu¹, K. Liu³⁹, K. Y. Liu²⁷, L. D. Liu³¹, P. L. Liu^{1,a}, Q. Liu⁴¹, S. B. Liu^{46,a}, X. Liu²⁶, Y. B. Liu³⁰, Z. A. Liu^{1,a}, Zhiqing Liu²², H. Loehner²⁵, X. C. Lou^{1,a,h}, H. J. Lu¹⁷, J. G. Lu^{1,a}, Y. Lu¹, Y. P. Lu^{1,a}, C. L. Luo²⁸, M. X. Luo⁵², T. Luo⁴², X. L. Luo^{1,a}, X. R. Lyu⁴¹, F. C. Ma²⁷, H. L. Ma¹, L. L. Ma³³, M. M. Ma¹, Q. M. Ma¹, T. Ma¹, X. N. Ma³⁰, X. Y. Ma^{1,a}, Y. M. Ma³³, F. E. Maas¹⁴, M. Maggiora^{49A,49C}, Y. J. Mao³¹, Z. P. Mao¹, S. Marcello^{49A,49C}, J. G. Messchendorp²⁵, J. Min^{1,a}, R. E. Mitchell¹⁹, X. H. Mo^{1,a}, Y. J. Mo⁶, C. Morales Morales¹⁴, N. Yu. Muchnoi^{9,f}, H. Muramatsu⁴³, Y. Nefedov²³, F. Nerling¹⁴, I. B. Nikolaev^{9,f}, Z. Ning^{1,a}, S. Nisar⁸, S. L. Niu^{1,a}, X. Y. Niu¹, S. L. Olsen³², Q. Ouyang^{1,a}, S. Pacetti^{20B}, Y. Pan^{46,a}, P. Patteri^{20A}, M. Pelizaeus⁴, H. P. Peng^{46,a}, K. Peters¹⁰, J. Pettersson⁵⁰, J. L. Ping²⁸, R. G. Ping¹, R. Poling⁴³, V. Prasad¹, H. R. Qi², M. Qi²⁹, S. Qian^{1,a}, C. F. Qiao⁴¹, L. Q. Qin³³, N. Qin⁵¹, X. S. Qin¹, Z. H. Qin^{1,a}, J. F. Qiu¹, K. H. Rashid⁴⁸, C. F. Redmer²², M. Ripka²², G. Rong¹, Ch. Rosner¹⁴, X. D. Ruan¹², A. Sarantsev^{23,g}, M. Savrié^{21B}, K. Schoenning⁵⁰, S. Schumann²², W. Shan³¹, M. Shao^{46,a}, C. P. Shen², P. X. Shen³⁰, X. Y. Shen¹, H. Y. Sheng¹, M. Shi¹, W. M. Song¹, X. Y. Song¹, S. Sosio^{49A,49C}, S. Spataro^{49A,49C}, G. X. Sun¹, J. F. Sun¹⁵, S. S. Sun¹, X. H. Sun¹, Y. J. Sun^{46,a}, Y. Z. Sun¹, Z. J. Sun^{1,a}, Z. T. Sun¹⁹, C. J. Tang³⁶, X. Tang¹, I. Tapan^{40C}, E. H. Thorndike⁴⁴, M. Tiemens²⁵, M. Ullrich²⁴, I. Uman^{40D}, G. S. Varner⁴², B. Wang³⁰, B. L. Wang⁴¹, D. Wang³¹, D. Y. Wang³¹, K. Wang^{1,a}, L. L. Wang¹, L. S. Wang¹, M. Wang³³, P. Wang¹, P. L. Wang¹, S. G. Wang³¹, W. Wang^{1,a}, W. P. Wang^{46,a}, X. F. Wang³⁹, Y. Wang³⁷, Y. D. Wang¹⁴, Y. F. Wang^{1,a}, Y. Q. Wang²², Z. Wang^{1,a}, Z. G. Wang^{1,a}, Z. H. Wang^{46,a}, Z. Y. Wang¹, Z. Y. Wang¹, T. Weber²², D. H. Wei¹¹, J. B. Wei³¹, P. Weidenkaff²², S. P. Wen¹, U. Wiedner⁴, M. Wolke⁵⁰, L. H. Wu¹, L. J. Wu¹, Z. Wu^{1,a}, L. Xia^{46,a}, L. G. Xia³⁹, Y. Xia¹⁸, D. Xiao¹, H. Xiao⁴⁷, Z. J. Xiao²⁸, Y. G. Xie^{1,a}, Q. L. Xiu^{1,a}, G. F. Xu¹, J. J. Xu¹, L. Xu¹, Q. J. Xu¹³, Q. N. Xu⁴¹, X. P. Xu³⁷, L. Yan^{49A,49C}, W. B. Yan^{46,a}, W. C. Yan^{46,a}, Y. H. Yan¹⁸, H. J. Yang³⁴, H. X. Yang¹, L. Yang⁵¹, Y. X. Yang¹¹, M. Ye^{1,a}, M. H. Ye⁷, J. H. Yin¹, B. X. Yu^{1,a}, C. X. Yu³⁰, J. S. Yu²⁶, C. Z. Yuan¹, W. L. Yuan²⁹, Y. Yuan¹, A. Yuncu^{40B,c}, A. A. Zafar⁴⁸, A. Zallo^{20A}, Y. Zeng¹⁸, Z. Zeng^{46,a}, B. X. Zhang¹, B. Y. Zhang^{1,a}, C. Zhang²⁹, C. C. Zhang¹, D. H. Zhang¹, H. H. Zhang³⁸, H. Y. Zhang^{1,a}, J. Zhang¹, J. J. Zhang¹, J. L. Zhang¹, J. Q. Zhang¹, J. W. Zhang^{1,a}, J. Y. Zhang¹, J. Z. Zhang¹, K. Zhang¹, L. Zhang¹, S. Q. Zhang³⁰, X. Y. Zhang³³, Y. Zhang¹, Y. H. Zhang^{1,a}, Y. N. Zhang⁴¹, Y. T. Zhang^{46,a}, Yu Zhang⁴¹, Z. H. Zhang⁶, Z. P. Zhang⁴⁶, Z. Y. Zhang⁵¹, G. Zhao¹, J. W. Zhao^{1,a}, J. Y. Zhao¹, J. Z. Zhao^{1,a}, Lei Zhao^{46,a}, Ling Zhao¹, M. G. Zhao³⁰, Q. Zhao¹, Q. W. Zhao¹, S. J. Zhao⁵³, T. C. Zhao¹, Y. B. Zhao^{1,a}, Z. G. Zhao^{46,a}, A. Zhemchugov^{23,d}, B. Zheng⁴⁷, J. P. Zheng^{1,a}, W. J. Zheng³³, Y. H. Zheng⁴¹, B. Zhong²⁸,

L. Zhou^{1,a}, X. Zhou⁵¹, X. K. Zhou^{46,a}, X. R. Zhou^{46,a}, X. Y. Zhou¹, K. Zhu¹, K. J. Zhu^{1,a}, S. Zhu¹, S. H. Zhu⁴⁵,
X. L. Zhu³⁹, Y. C. Zhu^{46,a}, Y. S. Zhu¹, Z. A. Zhu¹, J. Zhuang^{1,a}, L. Zotti^{49A,49C}, B. S. Zou¹, J. H. Zou¹

(BESIII Collaboration)

- ¹ *Institute of High Energy Physics, Beijing 100049, People's Republic of China*
² *Beihang University, Beijing 100191, People's Republic of China*
³ *Beijing Institute of Petrochemical Technology, Beijing 102617, People's Republic of China*
⁴ *Bochum Ruhr-University, D-44780 Bochum, Germany*
⁵ *Carnegie Mellon University, Pittsburgh, Pennsylvania 15213, USA*
⁶ *Central China Normal University, Wuhan 430079, People's Republic of China*
⁷ *China Center of Advanced Science and Technology, Beijing 100190, People's Republic of China*
⁸ *COMSATS Institute of Information Technology, Lahore, Defence Road, Off Raiwind Road, 54000 Lahore, Pakistan*
⁹ *G.I. Budker Institute of Nuclear Physics SB RAS (BINP), Novosibirsk 630090, Russia*
¹⁰ *GSI Helmholtzcentre for Heavy Ion Research GmbH, D-64291 Darmstadt, Germany*
¹¹ *Guangxi Normal University, Guilin 541004, People's Republic of China*
¹² *GuangXi University, Nanning 530004, People's Republic of China*
¹³ *Hangzhou Normal University, Hangzhou 310036, People's Republic of China*
¹⁴ *Helmholtz Institute Mainz, Johann-Joachim-Becher-Weg 45, D-55099 Mainz, Germany*
¹⁵ *Henan Normal University, Xinxiang 453007, People's Republic of China*
¹⁶ *Henan University of Science and Technology, Luoyang 471003, People's Republic of China*
¹⁷ *Huangshan College, Huangshan 245000, People's Republic of China*
¹⁸ *Hunan University, Changsha 410082, People's Republic of China*
¹⁹ *Indiana University, Bloomington, Indiana 47405, USA*
²⁰ *(A)INFN Laboratori Nazionali di Frascati, I-00044, Frascati, Italy; (B)INFN and University of Perugia, I-06100, Perugia, Italy*
²¹ *(A)INFN Sezione di Ferrara, I-44122, Ferrara, Italy; (B)University of Ferrara, I-44122, Ferrara, Italy*
²² *Johannes Gutenberg University of Mainz, Johann-Joachim-Becher-Weg 45, D-55099 Mainz, Germany*
²³ *Joint Institute for Nuclear Research, 141980 Dubna, Moscow region, Russia*
²⁴ *Justus Liebig University Giessen, II. Physikalisches Institut, Heinrich-Buff-Ring 16, D-35392 Giessen, Germany*
²⁵ *KVI-CART, University of Groningen, NL-9747 AA Groningen, The Netherlands*
²⁶ *Lanzhou University, Lanzhou 730000, People's Republic of China*
²⁷ *Liaoning University, Shenyang 110036, People's Republic of China*
²⁸ *Nanjing Normal University, Nanjing 210023, People's Republic of China*
²⁹ *Nanjing University, Nanjing 210093, People's Republic of China*
³⁰ *Nankai University, Tianjin 300071, People's Republic of China*
³¹ *Peking University, Beijing 100871, People's Republic of China*
³² *Seoul National University, Seoul, 151-747 Korea*
³³ *Shandong University, Jinan 250100, People's Republic of China*
³⁴ *Shanghai Jiao Tong University, Shanghai 200240, People's Republic of China*
³⁵ *Shanxi University, Taiyuan 030006, People's Republic of China*
³⁶ *Sichuan University, Chengdu 610064, People's Republic of China*
³⁷ *Soochow University, Suzhou 215006, People's Republic of China*
³⁸ *Sun Yat-Sen University, Guangzhou 510275, People's Republic of China*
³⁹ *Tsinghua University, Beijing 100084, People's Republic of China*
⁴⁰ *(A)Istanbul Aydin University, 34295 Sefakoy, Istanbul, Turkey; (B)Istanbul Bilgi University, 34060 Eyup, Istanbul, Turkey; (C)Uludag University, 16059 Bursa, Turkey; (D)Near East University, Nicosia, North Cyprus, 10, Mersin, Turkey*
⁴¹ *University of Chinese Academy of Sciences, Beijing 100049, People's Republic of China*
⁴² *University of Hawaii, Honolulu, Hawaii 96822, USA*
⁴³ *University of Minnesota, Minneapolis, Minnesota 55455, USA*
⁴⁴ *University of Rochester, Rochester, New York 14627, USA*
⁴⁵ *University of Science and Technology Liaoning, Anshan 114051, People's Republic of China*

⁴⁶ *University of Science and Technology of China, Hefei 230026, People's Republic of China*

⁴⁷ *University of South China, Hengyang 421001, People's Republic of China*

⁴⁸ *University of the Punjab, Lahore-54590, Pakistan*

⁴⁹ (A) *University of Turin, I-10125, Turin, Italy; (B) University of Eastern Piedmont, I-15121, Alessandria, Italy; (C) INFN, I-10125, Turin, Italy*

⁵⁰ *Uppsala University, Box 516, SE-75120 Uppsala, Sweden*

⁵¹ *Wuhan University, Wuhan 430072, People's Republic of China*

⁵² *Zhejiang University, Hangzhou 310027, People's Republic of China*

⁵³ *Zhengzhou University, Zhengzhou 450001, People's Republic of China*

^a *Also at State Key Laboratory of Particle Detection and Electronics, Beijing 100049, Hefei 230026, People's Republic of China*

^b *Also at Ankara University, 06100 Tandogan, Ankara, Turkey*

^c *Also at Bogazici University, 34342 Istanbul, Turkey*

^d *Also at the Moscow Institute of Physics and Technology, Moscow 141700, Russia*

^e *Also at the Functional Electronics Laboratory, Tomsk State University, Tomsk, 634050, Russia*

^f *Also at the Novosibirsk State University, Novosibirsk, 630090, Russia*

^g *Also at the NRC "Kurchatov Institute", PNPI, 188300, Gatchina, Russia*

^h *Also at University of Texas at Dallas, Richardson, Texas 75083, USA*

ⁱ *Also at Istanbul Arel University, 34295 Istanbul, Turkey*

The spin and parity of the $Z_c(3900)^\pm$ state are determined to be $J^P = 1^+$ with a statistical significance larger than 7σ over other quantum numbers in a partial wave analysis of the process $e^+e^- \rightarrow \pi^+\pi^-J/\psi$. We use a data sample of 1.92 fb^{-1} accumulated at $\sqrt{s} = 4.23$ and 4.26 GeV with the BESIII experiment. When parameterizing the $Z_c(3900)^\pm$ with a Flatté-like formula, we determine its pole mass $M_{\text{pole}} = (3881.2 \pm 4.2_{\text{stat}} \pm 52.7_{\text{syst}}) \text{ MeV}/c^2$ and pole width $\Gamma_{\text{pole}} = (51.8 \pm 4.6_{\text{stat}} \pm 36.0_{\text{syst}}) \text{ MeV}$. We also measure cross sections for the process $e^+e^- \rightarrow Z_c(3900)^+\pi^- + c.c. \rightarrow J/\psi\pi^+\pi^-$ and determine an upper limit at the 90% confidence level for the process $e^+e^- \rightarrow Z_c(4020)^+\pi^- + c.c. \rightarrow J/\psi\pi^+\pi^-$.

PACS numbers: 14.40.Rt, 13.66.Bc, 14.40.Pq

A charged charmoniumlike state, Z_c^\pm (Z_c denotes $Z_c(3900)$ throughout this Letter except when its mass is explicitly mentioned), was observed by the BESIII [1] and Belle [2] collaborations in the process $e^+e^- \rightarrow \pi^+\pi^-J/\psi$ and confirmed using CLEO-c's data [3]. As there are at least four quarks in the structure, many theoretical interpretations of the nature and the decay dynamics of the Z_c have been put forward [4–9].

A similar charged structure, the $Z_c(3885)^\pm$, was observed in the process $e^+e^- \rightarrow (D\bar{D}^*)^\pm\pi^\mp$ [10], with spin parity (J^P) assignment of 1^+ favored over the 1^- and 0^- hypotheses. However, its mass and width are 2σ and 1σ , respectively, below those of the Z_c^\pm observed in $e^+e^- \rightarrow \pi^+\pi^-J/\psi$. Are the $Z_c(3885)^\pm$ and the Z_c^\pm the same state and do they have the same spin and parity? This is one of the most important piece of information desired in many theoretical analyses [6, 11]. Finally, the $Z_c(4020)$ was observed for the first time in the processes $e^+e^- \rightarrow \pi^+\pi^-h_c$ [12] and $e^+e^- \rightarrow (D^*\bar{D}^*)^\pm\pi^\mp$ [13], but it has not been searched for in the $\pi^+\pi^-J/\psi$ final state yet.

In this Letter, we report on the determination of spin and parity of the Z_c and a search for the $Z_c(4020)^\pm$ in

the process $e^+e^- \rightarrow \pi^+\pi^-J/\psi$. The results are based on a partial wave analysis (PWA) of the $e^+e^- \rightarrow \pi^+\pi^-J/\psi$ events accumulated with the BESIII detector [14]. The data sample includes 1092 pb^{-1} e^+e^- collision data at a center-of-mass (c.m.) energy $\sqrt{s} = 4.23 \text{ GeV}$, and 827 pb^{-1} data at $\sqrt{s} = 4.26 \text{ GeV}$ [15]. The precise c.m. energies are measured with the di-muon process [16].

The $e^+e^- \rightarrow \pi^+\pi^-J/\psi$ candidate events are selected with the same selection criteria as described in Ref. [1, 17] with J/ψ reconstructed from lepton pairs ($\ell^+\ell^- = \mu^+\mu^-$, e^+e^-). The numbers of selected candidate events are 4154 at $\sqrt{s} = 4.23 \text{ GeV}$ and 2447 at $\sqrt{s} = 4.26 \text{ GeV}$; the event samples are estimated to contain 365 and 272 background events, respectively, at these two points, using the J/ψ mass sidebands as has been done in Ref. [1].

Amplitudes of the PWA are constructed with the helicity-covariant method [18]; the process $e^+e^- \rightarrow \pi^+\pi^-J/\psi$ is assumed to proceed via the Z_c resonance, *i.e.*, $e^+e^- \rightarrow Z_c^\pm\pi^\mp$, $Z_c^\pm \rightarrow J/\psi\pi^\pm$, and via the non- Z_c decay $e^+e^- \rightarrow R J/\psi$, $R \rightarrow \pi^+\pi^-$. All processes are added coherently to obtain the total amplitude [19]. For a particle decaying to the two-body final state, *i.e.*,

$A(J, m) \rightarrow B(s, \lambda)C(\sigma, \nu)$, where spin and helicity are indicated in the parentheses, its helicity amplitude $F_{\lambda, \nu}$ is related to the covariant amplitude via [18, 20]

$$F_{\lambda, \nu} = \sum_{lS} g_{lS} \sqrt{\frac{2l+1}{2J+1}} \langle l0S\delta | J\delta \rangle \langle s\lambda\sigma - \nu | S\delta \rangle r^l \frac{B_l(r)}{B_l(r_0)}, \quad (1)$$

where $\delta = \lambda - \nu$, and g_{lS} is the coupling constant in the l - S coupling scheme, the angular brackets denote Clebsch-Gordan coefficients, r is the magnitude of the momentum difference between the two final state particles, r_0 corresponds to the momentum difference at the nominal mass of the resonance, and B_l is a barrier factor [21]. The nonresonant process, $e^+e^- \rightarrow \pi^+\pi^- J/\psi$, is parameterized with an amplitude based on the QCD multipole expansion [22].

The relative magnitudes and phases of the complex coupling constants g_{lS} are determined by an unbinned maximum likelihood fit to data. The minimization is performed using the package MINUIT [23], and the backgrounds are subtracted from the likelihood as in Ref. [24].

In the nominal fit, we assume the Z_c to have $J^P = 1^+$, and its lineshape is described with a Flatté-like formula taking into account the fact that the Z_c^\pm decays are dominated by the final states $(D\bar{D}^*)^\pm$ [10] and $J/\psi\pi^\pm$ [1], *i.e.*,

$$BW(s, M, g'_1, g'_2) = \frac{1}{s - M^2 + i[g'_1\rho_1(s) + g'_2\rho_2(s)]}, \quad (2)$$

where the subscripts in g'_i ($i = 1, 2$) represent the $Z_c^\pm \rightarrow \pi^\pm J/\psi$ and $(D\bar{D}^*)^\pm$ decays, respectively; $\rho_i(s) = 2k_i/\sqrt{s}$ is a kinematic factor with k_i being the magnitude of the three-vector momentum of the final state particle (J/ψ or D) in the Z_c rest frame; and g'_1 and g'_2 are the coupling strengths of $Z_c^\pm \rightarrow \pi^\pm J/\psi$ and $Z_c^\pm \rightarrow (D\bar{D}^*)^\pm$, respectively, which will be determined by the fit to data.

To describe the $\pi^+\pi^-$ mass spectrum, four resonances, σ , $f_0(980)$, $f_2(1270)$ and $f_0(1370)$, are introduced. $f_0(980)$ is described with a Flatté formula [25], and the others are described with relativistic Breit-Wigner (BW) functions. The width of the wide resonance σ is parameterized with $\Gamma_\sigma(s) = \sqrt{1 - \frac{4m_\pi^2}{s}} \Gamma$ [26, 27], and the masses and widths for the $f_2(1270)$ and $f_0(1370)$ are taken from the Particle Data Group (PDG) [28]. The statistical significance for each resonance is determined by examining the probability of the change in log likelihood ($\log L$) values between including and excluding this resonance in the fits, and the probability is calculated under the χ^2 distribution hypothesis taking the change of the number of degrees of freedom $\Delta(\text{ndf})$ into account. With this procedure, the statistical significance of each of these states and the nonresonant process is estimated to be larger than 5σ . All of them are therefore included in the nominal fit, which includes the $e^+e^- \rightarrow \sigma J/\psi$,

$f_0 J/\psi$, $f_0(1370) J/\psi$, $f_2(1270) J/\psi$, $Z_c^\pm \pi^\mp$ and nonresonant processes.

A simultaneous fit is performed to the two data sets. The coupling constants are set as free parameters and are allowed to be different at the two energy points except for the common ones describing Z_c decays. The oppositely charged Z_c states are regarded as isospin partners; they share a common mass and coupling parameters g'_1 and g'_2 . Figure 1 shows projections of the fit results at $\sqrt{s} = 4.23$ and 4.26 GeV. The mass of Z_c^\pm is measured to be $M_{Z_c} = (3901.5 \pm 2.7_{\text{stat}})$ MeV/ c^2 and the coupling parameters $g'_1 = (0.075 \pm 0.006_{\text{stat}})$ GeV² and $g'_2/g'_1 = 27.1 \pm 2.0_{\text{stat}}$. This measurement is consistent with the previous result $g'_2/g'_1 = 27.1 \pm 13.1$ estimated based on the measured decay width ratio $\Gamma(Z_c^\pm \rightarrow (D\bar{D}^*)^\pm)/\Gamma(Z_c^\pm \rightarrow J/\psi\pi^\pm) = 6.2 \pm 2.9$ [10]. If the Z_c^\pm is parameterized as a constant width BW function, the simultaneous fit gives a mass of $(3897.6 \pm 1.2_{\text{stat}})$ MeV/ c^2 and a width of $(43.5 \pm 1.5_{\text{stat}})$ MeV, but the value of $-\ln L$ increases by 22 with $\Delta(\text{ndf}) = 1$. The BW parametrization is thus disfavored with a significance of 6.6σ .

Figure 2 shows the polar angle ($\theta_{Z_c^\pm}$) distribution of Z_c^\pm in the process $e^+e^- \rightarrow Z_c^+\pi^- + c.c.$ and the helicity angle ($\theta_{J/\psi}$) distribution in the decay $Z_c^\pm \rightarrow \pi^\pm J/\psi$ for the combined data within the Z_c mass region $m_{J/\psi\pi^\pm} \in (3.86, 3.92)$ GeV/ c^2 , where $\theta_{J/\psi}$ is the angle between the momentum of J/ψ in the Z_c rest frame and the Z_c momentum in the e^+e^- rest frame. The fit results, using different assumptions for the Z_c spin and parity, are drawn with a global normalization factor. The distribution indicates that data favors a spin and parity assignment of 1^+ for the Z_c^\pm . The significance of the $Z_c^\pm(1^+)$ hypothesis is further examined using the hypothesis test [29], in which the alternative hypothesis is our nominal fit with an additional $Z_c^\pm(J^P \neq 1^+)$ state. Possible J^P assignments, other than 1^+ , are 0^- , 1^- , 2^- , and 2^+ . The changes $-2\Delta \ln L$ when the $Z_c(1^+)\pi^\mp$ amplitude is removed from the alternative hypothesis are listed in Table I. Using the associated change in the ndf when the $Z_c^\pm(1^+)$ is excluded, we determine the significance of the 1^+ hypothesis over the alternative J^P possibilities to be larger than 7σ .

The fit results shown in Fig. 1 indicate that process is dominated by the $\pi\pi$ S -wave resonances, *i.e.* the σ , $f_0(980)$ and $f_0(1370)$. The fraction of all $\pi^+\pi^-$ S -wave components including the interference between them is measured to be $(61.7 \pm 2.1_{\text{stat}})\%$ of the total $\pi^+\pi^- J/\psi$ events at $\sqrt{s} = 4.23$ GeV and $(71.4 \pm 4.1_{\text{stat}})\%$ at $\sqrt{s} = 4.26$ GeV. The signal yields $N_{Z_c^\pm}$ of Z_c^\pm are calculated by scaling its partial signal ratio with the total number of signal events. They are measured to be $N_{Z_c^\pm} = 952.3 \pm 39.3_{\text{stat}}$ at $\sqrt{s} = 4.23$ GeV and $343.3 \pm 23.3_{\text{stat}}$ at $\sqrt{s} = 4.26$ GeV. Here, the errors are statistical only, and they are estimated using the covariance matrix from the fits.

To measure amplitudes associated with the polariza-

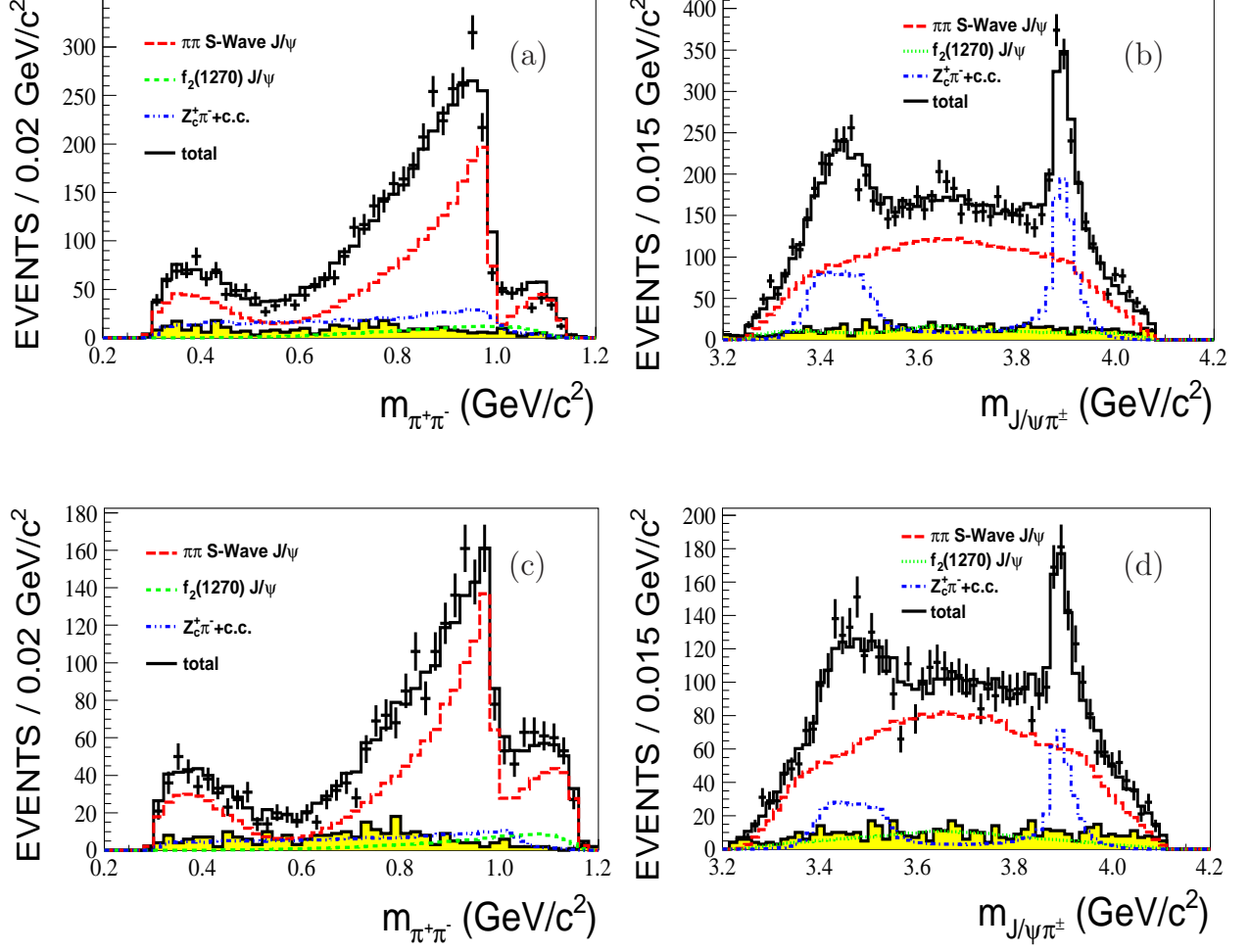


FIG. 1: (color online) Projections to $m_{\pi^+\pi^-}$ (a, c) and $m_{J/\psi\pi^\pm}$ (b, d) of the fit results with $J^P = 1^+$ for the Z_c , at $\sqrt{s} = 4.23$ GeV (a, b) and $\sqrt{s} = 4.26$ GeV (c, d). The points with error bars are data, and the black histograms are the total fit results including backgrounds. The shaded histogram denotes backgrounds. The contributions from the $\pi^+\pi^-$ S -wave J/ψ , $f_2(1270)J/\psi$, and $Z_c^\pm\pi^\mp$, are shown in the plots. The $\pi^+\pi^-$ S -wave resonances include the σ , $f_0(980)$ and $f_0(1370)$. Plots (b) and (d) are filled with two entries ($m_{J/\psi\pi^+}$ and $m_{J/\psi\pi^-}$) per event.

tion of Z_c^\pm in $e^+e^- \rightarrow Z_c^\pm\pi^\mp$ and that of J/ψ in $Z_c^\pm \rightarrow J/\psi\pi^\pm$ decays in the nominal fit, the ratios of helicity amplitudes with different polarizations as defined in Eq. (1) are calculated to be $|F_{1,0}^{Z_c}|^2/|F_{0,0}^{Z_c}|^2 = 0.22 \pm 0.05_{\text{stat}}$ at 4.23 GeV, and $0.21 \pm 0.11_{\text{stat}}$ at 4.26 GeV for $e^+e^- \rightarrow Z_c^\pm\pi^\mp$, and $|F_{1,0}^{J/\psi}|^2/|F_{0,0}^{J/\psi}|^2 = 0.45 \pm 0.15_{\text{stat}}$ for $Z_c^\pm \rightarrow J/\psi\pi^\pm$, at both energy points. Here $F_{1,0}^{Z_c/J/\psi}$ and $F_{0,0}^{Z_c/J/\psi}$ correspond to transverse and longitudinal polarization amplitudes in the decay, respectively. The results show that the Z_c polarization is dominated by the longitudinal component.

The Born cross section for Z_c production is measured with the relation $\sigma = N_{Z_c^\pm}/(\mathcal{L}(1+\delta)\epsilon\mathcal{B})$, where $N_{Z_c^\pm}$ is the signal yield for the process $e^+e^- \rightarrow Z_c^+\pi^- + c.c. \rightarrow \pi^+\pi^- J/\psi$, \mathcal{L} is the integrated luminosity, and ϵ is the

detection efficiency obtained from a MC simulation which is generated using the amplitude parameters determined in the PWA. The radiative correction factor $(1+\delta)$ is determined to be 0.818 [1]. The Born cross section is measured to be $(22.0 \pm 1.0_{\text{stat}})$ pb at $\sqrt{s} = 4.23$ GeV and $(11.0 \pm 1.2_{\text{stat}})$ pb at $\sqrt{s} = 4.26$ GeV.

Using these two data sets, we also search for the process $e^+e^- \rightarrow Z_c(4020)^+\pi^- + c.c. \rightarrow \pi^+\pi^- J/\psi$, with the $Z_c(4020)^\pm$ assumed to be a 1^+ state. In the PWA, its mass is taken from Ref. [12], and its width is taken as the observed value, which includes the detector resolution. The statistical significance for $Z_c(4020)^\pm \rightarrow J/\psi\pi^\pm$ is found to be 3σ in the combined data. The Born cross sections are measured to be $(0.2 \pm 0.1_{\text{stat}})$ pb at 4.23 GeV and $(0.8 \pm 0.4_{\text{stat}})$ pb at $s = 4.26$ GeV, and the cor-

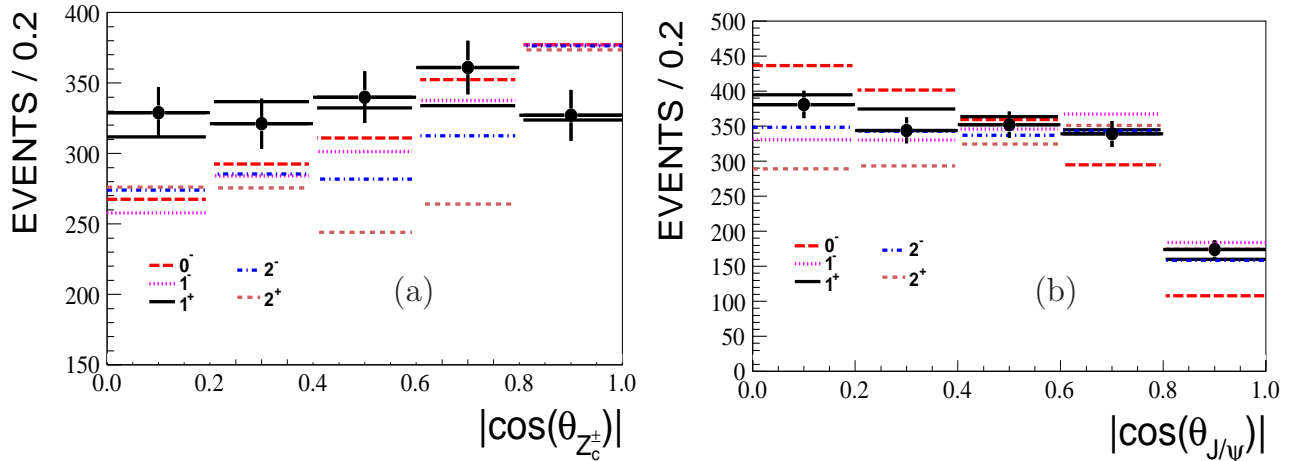


FIG. 2: (color online) (a) Polar angle distribution of Z_c^\pm in the process $e^+e^- \rightarrow Z_c^\pm \pi^\mp + c.c.$, (b) helicity angle distribution of J/ψ in the $Z_c^\pm \rightarrow \pi^\pm J/\psi$. The dots with error bars show the combined data with requirement $m_{J/\psi\pi^\pm} \in (3.86, 3.92)$ GeV/c^2 , and compared to the total fit results with different J^P hypotheses.

TABLE I: Significance of the spin parity 1^+ over other quantum numbers for Z_c^\pm . The significance is obtained for given change in ndf, $\Delta(\text{ndf})$. In each case, $\Delta(\text{ndf}) = 2 \times 4 + 5$, where 2×4 ndf account for the coupling strength for $e^+e^- \rightarrow Z_c^\pm \pi^\mp$ at the two data sets, and the additional five ndf are the contribution of the common degrees of freedom for the Z_c resonant parameters and the coupling strength for $Z_c^\pm \rightarrow J/\psi \pi^\pm$.

Hypothesis	$\Delta(-2 \ln L)$	$\Delta(\text{ndf})$	Significance
1^+ over 0^-	94.0	13	7.6σ
1^+ over 1^-	158.3	13	10.8σ
1^+ over 2^-	151.9	13	10.5σ
1^+ over 2^+	96.0	13	7.7σ

responding upper limits at the 90% confidence level are estimated to be 0.9 pb and 1.4 pb, respectively.

Systematic errors associated with the event selection, including the luminosity measurement, tracking efficiency of charged tracks, kinematic fit, initial state radiation (ISR) correction factor and the branching fraction of $Br(J/\psi \rightarrow \ell^+\ell^-)$, have been estimated to be 4.8% for the cross section measurement and 1.8 MeV for the Z_c mass in the previous analysis [1].

Uncertainties associated with the amplitude analysis come from the σ and Z_c parametrizations, the background estimation, the parameters in the $f_0(980)$ Flatté formula, the barrier radius in the barrier factor, the mass resolution and the component of non-resonant amplitude.

The systematic uncertainty due to the σ lineshape is estimated by comparing the nominal fit with two other parameterizations, the PKU ansatz [30] and the Zou-Bugg approach [31]. The differences in the Z_c signal

yields and mass measurement are taken as the errors, which are 2.5% (31.0%) for the signal yields at 4.23 (4.26) GeV and 19.5 MeV for the Z_c mass.

The uncertainty due to the $f_0(980)$ lineshape is estimated by varying the couplings by 1σ as determined in the decays $J/\psi \rightarrow \phi\pi^+\pi^-$ and ϕK^+K^- [25]. Uncertainties associated with the $f_0(1370)$ are estimated by varying the mass and width by one standard deviation around the world average values [28].

The uncertainty due to the Z_c parametrization is estimated by using a constant-width relativistic BW function. The simultaneous fit gives the Z_c mass of $(3897.6 \pm 1.2_{\text{stat}})$ MeV/c^2 and the width of $(43.5 \pm 1.5_{\text{stat}})$ MeV. The difference in the Z_c signal yields is 15.5% (7.9%) for the data taken at 4.23 (4.26) GeV.

The uncertainty due to the background level is estimated by changing the number of background events by 1σ around the nominal value, that is, ± 25 around 637 events.

The barrier radius is usually taken in the range $r_0 \in (0.25, 0.76)$ fm, with 0.6 fm being used in the nominal fit. Uncertainties at both ends are checked. For a conservative estimation, the radius $r_0 = 0.76$ fm, which results in the larger difference, is used to estimate the uncertainty.

The uncertainty due to the mass resolution in the $J/\psi\pi$ invariant mass is estimated with an unfolded Z_c width. A truth width is unfolded from the observed Z_c width using a relation determined by the MC simulation, and its difference from the unfolded width, $\delta\Gamma/\Gamma = \delta g'_1/g'_1$, is taken as the systematic uncertainty for the coupling constant g'_1 . The uncertainties in the signal yields and the Z_c mass are determined with the truth coupling constant.

The nonresonant process is described with a formula

derived from the QCD multipole expansion [22]. It includes the S - and D -wave components. The uncertainty associated with this amplitude is estimated by removing the insignificant D -wave component and using the S -wave component only.

Table II summarizes the systematic uncertainties. Assuming all of these sources are independent, the total systematic uncertainties are 38.0 MeV for the measurement of the Z_c mass, and 20.3% (49.2%) for the measurement of Z_c cross sections at $\sqrt{s} = 4.23$ (4.26) GeV.

In summary, with 1.92 fb^{-1} data taken at $\sqrt{s} = 4.23$ and 4.26 GeV, the Z_c^\pm state is studied with an amplitude fit to the $e^+e^- \rightarrow \pi^+\pi^-J/\psi$ samples, and its spin and parity have been determined to be 1^+ with a statistical significance larger than 7σ over other quantum numbers. The mass is measured to be $M_{Z_c} = (3901.5 \pm 2.7_{\text{stat}} \pm 38.0_{\text{syst}}) \text{ MeV}/c^2$ in the parametrization of a Flatté-like formula with parameters $g'_1 = 0.075 \pm 0.006_{\text{stat}} \pm 0.025_{\text{syst}} \text{ GeV}^2$, and $g'_2/g'_1 = 27.1 \pm 2.0_{\text{stat}} \pm 1.9_{\text{syst}}$, which corresponds to the Z_c pole mass $M_{\text{pole}} = (3881.2 \pm 4.2_{\text{stat}} \pm 52.7_{\text{syst}}) \text{ MeV}/c^2$ and pole width $\Gamma_{\text{pole}} = (51.8 \pm 4.6_{\text{stat}} \pm 36.0_{\text{syst}}) \text{ MeV}$, where $M_{\text{pole}} - i\Gamma_{\text{pole}}/2$ is the solution for which the denominator of Flatté-like formula is zero. The pole mass is consistent with the previous measurement [10]. The Born cross sections for the process $e^+e^- \rightarrow \pi^+Z_c^- + c.c.$ are measured to be $(21.8 \pm 1.0_{\text{stat}} \pm 4.4_{\text{syst}}) \text{ pb}$ at $\sqrt{s} = 4.23 \text{ GeV}$ and $(11.0 \pm 1.2_{\text{stat}} \pm 5.4_{\text{syst}}) \text{ pb}$ at $\sqrt{s} = 4.26 \text{ GeV}$. The contributions from $Z_c(4020)^\pm$ are also searched for, but no significant signals are observed, and an upper limit for the $e^+e^- \rightarrow \pi^+Z_c(4020)^- + c.c.$ process is determined to be 0.9 (1.4) pb at $\sqrt{s} = 4.23$ (4.26) GeV.

The BESIII collaboration thanks the staff of BEPCII and the computing center for their strong support. This work is supported in part by the Ministry of Science and Technology of China under Contract No. 2009CB825200; Joint Funds of the National Natural Science Foundation of China under Contracts Nos. U1332201; National Natural Science Foundation of China (NSFC) under Contracts Nos. 11175188, 11375205, 11235011, 11375221, 11565006, 10825524; German Research Foundation DFG under Contract No. Collaborative Research Center CRC-1044, 627240; Istituto Nazionale di Fisica Nucleare, Italy; Ministry of Development of Turkey under Contract No. DPT2006K-120470; U.S. Department of Energy under Contracts Nos. DE-SC-0012069, DE-SC-0010504, DE-SC-0010118, DE-FG02-05ER41374; U.S. National Science Foundation; University of Groningen (RuG) under Contracts No. 530-4CDP03, and the Helmholtzzentrum fuer Schwerionenforschung GmbH (GSI), Darmstadt; WCU Program of National Research Foundation of Korea under Contract No. R32-2008-000-10155-0.

- [2] Z. Q. Liu *et al.* (Belle Collaboration), Phys. Rev. Lett. **110**, 252002 (2013).
- [3] T. Xiao, S. Dobbs, A. Tomaradze and K. K. Seth, Phys. Lett. B **727**, 366 (2013).
- [4] N. Brambilla *et al.*, Eur. Phys. J. C **74**, 2981 (2014).
- [5] G. T. Bodwin *et al.*, arXiv:1307.7425.
- [6] M. B. Voloshin, Phys. Rev. D **87**, 091501(R) (2013).
- [7] A. Esposito *et al.*, Int. J. Mod. Phys. A **30**, 1530002 (2014).
- [8] X. Liu, Chin. Sci. Bull. **59**, 3815 (2014).
- [9] F.-K. Guo, C. Hidalgo-Duque, J. Nieves and M. Pavon Valderrama, Phys. Rev. D **88**, 054007 (2013).
- [10] M. Ablikim *et al.* (BESIII Collaboration), Phys. Rev. Lett. **112**, 022001 (2014).
- [11] E. Braaten, Phys. Rev. Lett. **111**, 162003 (2013).
- [12] M. Ablikim *et al.* (BESIII Collaboration), Phys. Rev. Lett. **111**, 242001 (2013).
- [13] M. Ablikim *et al.* (BESIII Collaboration), Phys. Rev. Lett. **112**, 132001 (2014).
- [14] M. Ablikim *et al.* (BESIII Collaboration), Nucl. Instrum. Meth. A **614**, 345 (2010).
- [15] M. Ablikim *et al.* (BESIII Collaboration), Chin. Phys. C **39**, 093001 (2015).
- [16] M. Ablikim *et al.* (BESIII Collaboration), Chin. Phys. C **40**, 063001 (2016).
- [17] M. Ablikim *et al.* (BESIII Collaboration), Phys. Rev. Lett. **118**, 092001 (2017).
- [18] S. U. Chung, Phys. Rev. D **57**, 431 (1998); S. U. Chung, Phys. Rev. D **48**, 1225 (1993); S. U. Chung and J. M. Friedrich, Phys. Rev. D **78**, 074027 (2008).
- [19] H. Chen and R. G. Ping, Phys. Rev. D **95**, 076010 (2017).
- [20] V. Filippini, A. Fontana and A. Rotondi, Phys. Rev. D **51**, 2247 (1995).
- [21] B. S. Zou and D. V. Bugg, Eur. Phys. J. A **16**, 537 (2003).
- [22] V. A. Novikov and M. A. Shifman, Z. Phys. C **8**, 43 (1981); M. B. Volshin, Prog. Part. Nucl. Phys. **61**, 455 (2008); D.-Y. Chen, X. Liu and X.-Q. Li, Eur. Phys. J. C **71**, 1808 (2011).
- [23] F. James, CERN Program Library Long Writeup D **506** (1998).
- [24] M. Ablikim *et al.* (BESIII Collaboration), Phys. Rev. D **86**, 072011 (2012).
- [25] M. Ablikim *et al.* (BES Collaboration), Phys. Lett. B **598**, 149 (2004).
- [26] S. M. Berman and M. Jacob, Phys. Rev. B **139**, 1608 (1965).
- [27] M. Ablikim *et al.* (BES Collaboration), Phys. Lett. B **645**, 19 (2007).
- [28] K. A. Olive *et al.* (Particle Data Group), Chin. Phys. C **38**, 090001 (2014).
- [29] I. Narsky, Nucl. Instrum. Meth. A **450**, 444 (2000); Y. S. Zhu, High Energy Physics and Nuclear Physics **30**, 331 (2006).
- [30] H. Q. Zheng *et al.*, Nucl. Phys. A **733**, 235 (2004).
- [31] B. S. Zou and D. V. Bugg, Phys. Rev. D **48**, 3948 (1993). M. Ablikim *et al.* (BES Collaboration), Phys. Lett. B, **598** 149 (2004).

[1] M. Ablikim *et al.* (BESIII Collaboration), Phys. Rev. Lett. **110**, 252001 (2013).

TABLE II: Summary of systematic uncertainties on the Z_c ($J^P = 1^+$) mass, parameters g'_1 and g'_2 , and the signal yields at 4.23 GeV ($N_{Z_c}^I$) and 4.26 GeV ($N_{Z_c}^{II}$). The uncertainties shown for the Z_c mass, parameter g'_1 and the ratio g'_2/g'_1 are absolute values, while the uncertainties for $N_{Z_c}^I$ and $N_{Z_c}^{II}$ are relative ones.

Sources	Z_c Mass (MeV/ c^2)	$g'_1 \times 10^3$ (GeV 2)	g'_2/g'_1	$N_{Z_c}^I$ (%)	$N_{Z_c}^{II}$ (%)
Event selection	1.8	4.8	4.8
σ lineshape	19.5	12.0	0.3	2.5	31.0
Z_c parametrization	3.9	15.5	7.9
Backgrounds	13.9	8.0	0.1	1.9	9.3
$f_0(980), g_1, g_2/g_1$	17.5	14.0	0.6	2.4	24.6
$f_0(1370)$	16.7	11.0	0.4	11.5	14.0
Barrier radius	7.9	2.0	1.7	0.5	12.9
Z_c mass resolution	1.0	2.0	...	0.4	0.5
Nonresonance	14.3	9.0	0.0	0.1	18.0
Total	38.0	24.8	1.9	20.3	49.2